o- and *m*-(Bromotetrafluorophenyl)palladium(II) Complexes: Atropisomerism Studies by ^{19}F NMR and Measurement of Through-Space F−F Coupling Constants

Ana C. Albéniz, Arturo L. Casado, and Pablo Espinet*

Departamento de Química Inorgánica, Facultad de Ciencias, Universidad de Valladolid, E-47005 Valladolid, Spain

Received June 23, 1997[⊗]

Palladium(II) complexes with the asymmetric aryl groups *o*-C_6BrF_4 and *m*-C_6BrF_4 have been synthesized, namely $[Pd_2(C_6BrF_4)_2(\mu\text{-}Cl)_2(tht)_2]$, *trans*-$[Pd(C_6BrF_4)Cl(tht)_2]$ (tht = tetrahydrothiophene), *trans*-$[Pd(C_6BrF_4)_2L_2]$, and *cis*-$[Pd(C_6BrF_4)_2L_2]$ (L_2 = 2tht, COD, Me_2-bipy (4,4′-dimethyl-2,2′-bipyridine), $OPPy_2Ph$ (Py = 2-pyridyl), $2PMe_3$, 2CNMe). A mixture of atropisomers (*syn*-*Br,Br* and *anti*-*Br,Br*) is found for most bis(aryl) complexes, and the ratio of *syn*:*anti* atropisomers depends upon the R group, the *cis* or *trans* geometry of the complexes, and the ancillary ligand: A ratio close to 1:1 is observed for the *cis*- and *trans*-*m*-C_6BrF_4 derivatives and for the *trans*-*o*-C_6BrF_4 complexes, but the *anti* atropisomer is preferred in the *cis*-*o*-C_6BrF_4 derivatives, particularly if the ancillary ligands extend out of the coordination plane. Strong through-space coupling between *syn* F_{ortho} atoms of mutually *cis* R groups is observed in the ^{19}F NMR spectra for *cis*-$[Pd(C_6BrF_4)_2L_2]$ complexes. *J*-values were determined which prove useful to unequivocally identify the atropisomers formed and to detect distortions in the structure of the complexes. Atropisomerization by aryl rotation is observed in several cases at different rates: Faster for *m*-C_6BrF_4 than for *o*-C_6BrF_4 derivatives, and faster for small-in-plane than for bulk-in-plane ancillary ligands. The fastest rotation occurs in the complexes with CNMe, which do not show atropisomers by ^{19}F NMR at room temperature.

Introduction

The use of highly symmetric aryl groups is advantageous for the identification of many organometallic compounds but can be a drawback in the study of certain dynamic processes. Thus, to study the aryl rotation about the M−R bond (M = Pd, Pt; R = C_6F_5), it is necessary to use ancillary ligands that render the two sides of the coordination plane inequivalent and make the rotation observable by the equivalence it produces. Recently, we proved that in complexes $[M(C_6F_5)X(OPPy_nPh_{3-n})]$ (Chart 1; M = Pd, Pt; X = C_6F_5, halide; n = 2, 3) there is a restricted rotation about the Pd−C_6F_5 bond in the square planar compound that makes the two halves of the C_6F_5 group equivalent.[1,2] In order to prove this rotation, we had to discount that the equivalence was produced by movements of the ligand. In fact, for one of the complexes (M = Pd; X = Cl; n = 3) the equivalence was observed at a faster rate and was due to associative substitution of the Py groups producing "inversion" of the chelating ligand (that is, this inversion produced an apparent rotation at a faster rate than the real rotation). Other ligand fluxional processes can also produce a deceptive effect of aryl rotation about the M−C bond.[3]

Chart 1

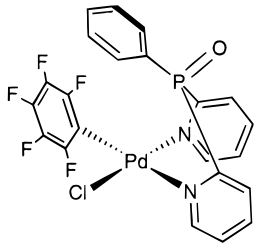

A way to overcome this uncertainty is to use nonsymmetrical *o*-C_6BrF_4 or *m*-C_6BrF_4 derivatives. The presence of atropisomers is unequivocally proof of restricted rotation, and the only way to produce atropisomerization is rotation about the M−C bond, so there is no need to disprove other mechanisms. Moreover, the rotation can also be observed in complexes where the coordination plane is a symmetry plane.

The *cis*-bis(bromotetrafluorophenyl)palladium derivatives described here display complex static ^{19}F NMR spectra. Their complete study shows that they contain inter-aryl (including fairly large through-space) F−F couplings between F atoms belonging to different groups in the same molecule. Through-space F−F coupling constants have been observed in many organic derivatives whose structures place these atoms at short

[⊗] Abstract published in *Advance ACS Abstracts,* December 1, 1997.

(1) Casares, J. A.; Coco, S.; Lin, L.-S.; Espinet, P. *Organometallics* **1995**, *14*, 3058−3067.

(2) Some other examples of restricted aryl rotation about the M−C bond are as follows: (a) Brown, J. M.; Pérez-Torrente, J.; Alcock, N. *Organometallics* **1995**, *14*, 1195−1203. (b) Rieger, A. L.; Carpenter, G. B.; Rieger, P. H. *Organometallics* **1993**, *12*, 842−847. (c) Selnau, H. E.; Merola, J. S. *Organometallics* **1993**, *12*, 1583−1591. (d) Alsters, P. L.; Boersma, J.; Smeets, W. J. J.; Spek, A. L.; Van Koten, G. *Organometallics* **1993**, *13*, 1639−1647. (e) Anderson, G. K.; Cross, R. J.; Manojlovic-Muir, L.; Muir, K. W.; Rocamora, M. *Organometallics* **1988**, *7*, 1520−1525. (f) Baumgärtner, R.; Brune, H.-A. *J. Organomet. Chem.* **1988**, *350*, 115−127. (g) Probitts, E. J.; Saunders, D. R.; Stone, M. H.; Mawby, R. J. *J. Chem. Soc. Dalton Trans.* **1986**, 1167−1173. (h) Jones, W. D.; Feher, F. J. *Inorg. Chem.* **1984**, *23*, 2376−2388. (i) Wada, M.; Sameshima, K. *J. Chem. Soc., Dalton Trans.* **1981**, 240−244.

(3) Abel, E. W.; Orrell, K. G.; Osborne, A. G.; Pain, H. M.; Sik, V.; Hursthouse, M. B.; Abdul Malik, K. M. *J. Chem. Soc., Dalton Trans.* **1994**, 3441−3449.

S0276-7333(97)00529-3 CCC: $14.00

distances.[4] However, although many *cis*-bis(fluorophenyl)metal derivatives have been reported so far,[5] this type of coupling, responsible in part for the complicated spin systems observed, had not been recognized before, except in one case where it was attributed to scalar four- or five-bond cross ring coupling.[3]

Results and Discussion

Synthesis. Complexes containing one or two bromotetrafluorophenyl groups bound to palladium were synthesized. The arylation reactions were carried out using convenient precursors for each stoichiometry and geometry. The reaction of *trans*-$[PdCl_2(tht)_2]$ (tht = tetrahydrothiophene) with LiR leads to mixtures of *trans*-$[PdR_2(tht)_2]$ (**1**) and *cis*-$[PdR_2(tht)_2]$ (**2**) (eq 1).

$$trans\text{-}[PdCl_2(tht)_2] + 2LiR \rightarrow [PdR_2(tht)_2] + 2LiCl \quad (1)$$

The *trans* to *cis* ratio depends on the aryl group: **1o**:**2o** = 9:1 (R = *o*-C_6BrF_4); **1m**:**2m** = 1:1 (R = *m*-C_6BrF_4). The *trans* and *cis* isomers can be separated as described in the Experimental Section. The *trans* complexes isomerize slowly in $CDCl_3$ solution to the corresponding *cis* isomers (eq 2), as observed before for the corresponding C_6F_5 or $C_6Cl_2F_3$ derivatives.[6,7] The process is first

$$trans\text{-}[PdR_2(tht)_2] \rightarrow cis\text{-}[PdR_2(tht)_2] \quad (2)$$

order in Pd complex, and the observed rate constants are $k_{iso} = 1.3 \times 10^{-6}$ s^{-1} for **1o** and $k_{iso} = 8.1 \times 10^{-6}$ s^{-1} for **1m** (10 mM solutions at 318.2 K). The ratios at equilibrium are **1o**:**2o** = 35:65; **1m**:**2m** = 4:96.

It is known that *trans*−*cis* isomerization during the arylation process is catalyzed by the aryllithium reagent via the formation of $[PdR_3L]^-$ intermediates.[8] The observed results suggest that the first product of the arylation of *trans*-$[PdCl_2(tht)_2]$ is *trans*-$[PdR_2(tht)_2]$ and that the catalysis of isomerization is less efficient for R = *o*-C_6BrF_4, probably because the formation of $[PdR_3L]^-$ is less favorable for *o*-C_6BrF_4 than for the less hindered *m*-C_6BrF_4 or C_6F_5.

Arylation of *cis*-$[PdCl_2(COD)]$ by organolithium reagents LiR leads to *cis*-$[PdR_2(COD)]$ (**3o**, R = *o*-C_6BrF_4; **3m**, R = *m*-C_6BrF_4). This synthetic approach (eq 3) was used previously for other R groups such as Me, C_6F_5, and 2,5-$C_6Cl_2F_3$.[5,6,9]

$$cis\text{-}[PdCl_2(COD)] + 2LiR \rightarrow cis\text{-}[PdR_2(COD)] + 2LiCl \quad (3)$$

Complex **3m** was obtained in higher yield (71%) than **3o** (59%). Moreover, depending on the reaction conditions used in the arylation reaction that produces **3o**, $[Pd_2(\mu\text{-}Cl)_2\{6\text{-}(o\text{-}C_6BrF_4)\text{-}\eta^3\text{-}cyclooct\text{-}1\text{-}en\text{-}5\text{-}yl\}_2]$ (**12**) could be isolated in 10% yield (see Experimental Section). The latter is formed by insertion of one double bond of COD into the Pd−R bond in the mono-arylated complex *cis*-$[Pd(o\text{-}C_6BrF_4)Cl(COD)]$, as reported for similar C_6F_5 complexes.[10] The insertion byproduct was not found in the preparation of **3m**. This suggests that, again for steric reasons, the second arylation of *cis*-$[Pd(o\text{-}C_6BrF_4)Cl(COD)]$ is much slower than that for the analogous derivative with *m*-C_6BrF_4 so that the insertion reaction can compete with it, decreasing the preparative yield in **3o**.

Complexes **1**, **2**, or **3** react fast with stoichiometric amounts of ligands, such as Me_2bipy (4,4′-dimethyl-2,2′-bipyridine), $OPPy_2Ph$ (Py = 2-pyridyl), PMe_3, or CNMe, to give new complexes $[Pd(C_6BrF_4)_2L'_2]$ (**4**−**9**, see Tables 1 and 2) which preserve the *cis* or *trans* geometry of the starting products (eq 4).

$$[PdR_2L_2] + 2L' \rightarrow [PdR_2L'_2] + 2L \quad (4)$$

All of the bis(bromotetrafluorophenyl)palladium complexes prepared (see Tables 1 and 2), except **5o**, **5m**, and **7m**, appear as a mixture of atropisomers *syn-Br,-Br* and *anti-Br,Br* at room temperature (Figure 1). For **9o** and **9m**, with an asymmetric ligand, the *syn-Br,Br* isomer is further split in two, depending on whether the Br and P substituents are in the same (*syn-Br,P*) or in opposite (*anti-Br,P*) faces of the palladium coordination plane. This gives a total of three observable atropisomers: Two *syn-Br,Br* and one *anti-Br,Br*, which becomes chiral racemic. Other possible conformers with the oxygen atom toward Pd have not been detected. The conformation with the phenyl group close to Pd is proposed according to the structure found for the analogous C_6F_5 complex (Chart 1).[1]

The atropisomer ratio depends both on the *cis* or *trans* geometry and on the aryl group of the complexes. Ratios of 1:1, or very close to this value, are found for *trans*-$[Pd(m\text{-}C_6BrF_4)_2L_2]$, *trans*-$[Pd(o\text{-}C_6BrF_4)_2L_2]$, and *cis*-$[Pd(m\text{-}C_6BrF_4)_2L_2]$. In contrast, for the complexes *cis*-$[Pd(o\text{-}C_6BrF_4)_2L_2]$, the *anti-Br,Br* diastereoisomer is more abundant and the difference increases for ligands that extend out of the coordination plane. These abundances correspond to the equilibrium distribution (atropisomerization is fast compared to the preparative times) and reflect the influence of the Br substituent on the stability of the complexes: Unnoticeable for the *m*-C_6BrF_4 derivatives but important for the hindered *o*-C_6BrF_4 derivatives, making the most crowded *syn-Br,-Br* atropisomer less stable.

In order to help with the assignment of the ^{19}F NMR spectral patterns for the bis-arylated complexes, deriva-

(4) (a) Ernst, L.; Ibrom, K. *Angew. Chem., Int. Ed. Engl.* **1995**, *34*, 1881−1882. (b) Ernst, L.; Ibrom, K.; Marat, K.; Mitchell, R. H.; Bodwell, G. J.; Bushnell, G. W. *Chem. Ber.* **1994**, *127*, 1119−1124. (c) Lyga, J. W.; Henrie, R. N.; Meier, G. A.; Creekmore, R. W.; Patera, R. M. *Magn. Reson. Chem.* **1993**, *31*, 323−328. (d) Gribble, G. W.; Olson, E. R. *J. Org. Chem.* **1993**, *58*, 1631−1634. (e) Mallory, F. B.; Mallory, C. W. *J. Am. Chem. Soc.* **1985**, *107*, 4816−4819. (f) Mallory, F. B.; Mallory, C. W.; Ricker, W. M. *J. Am. Chem. Soc.* **1975**, *97*, 4770−4771 and references therein. (g) Mallory, F. B. *J. Am. Chem. Soc.* **1973**, *95*, 7747−7752 and references therein.

(5) (a) García, M. P.; Jiménez, M. V.; Lahoz, F. S.; Oro, L. A. *Inorg. Chem.* **1995**, *34*, 2153−2159. (b) Usón, R.; Forniés, J.; Falvello, L. R.; Tomás, M.; Casas, J. M.; Martín, A.; Cotton, F. A. *J. Am. Chem. Soc.* **1994**, *116*, 7160−7165. (c) Falvello, L. R.; Forniés, J.; Fortuño, C.; Martínez, F. *Inorg. Chem.* **1994**, *33*, 6242−6246. (d) López, G.; Ruiz, J.; García, G.; Vicente, C.; Casabó, J.; Molins, E.; Miravitlles, C. *Inorg. Chem.* **1991**, *30*, 2605−2610. (e) Usón, R.; Forniés, J. *Adv. Organomet. Chem.* **1988**, *28*, 219−297. (f) Deacon, G. B.; Nelson-Reed, K. T. *J. Organomet. Chem.* **1987**, *322*, 257−268.

(6) Espinet, P.; Martínez-Ilarduya, J. M.; Pérez-Briso, C.; Casado, A. L.; Alonso, M. A. *J. Organomet. Chem.*, in press.

(7) Minniti, D. *Inorg Chem.* **1994**, *33*, 2631−2634.

(8) Ozawa, F.; Kurihara, K.; Yamamoto, T.; Yamamoto, A. *J. Organomet. Chem.* **1985**, *279*, 233−243.

(9) Rudler-Chaurin, M.; Rudler, H. *J. Organomet. Chem.* **1977**, *134*, 115−119.

(10) Albéniz, A. C.; Espinet, P.; Jeannin, Y.; Philoche-Levisalles, M.; Mann, B. E. *J. Am. Chem. Soc.* **1990**, *112*, 6594−6600.

Table 1. ^{19}F NMR Data for (*o*-Bromotetrafluorophenyl)palladium(II) Complexes[a]

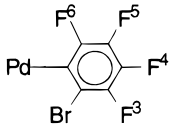

no.	complex[b]	atropisomer	%	δ_3	δ_4	δ_5	δ_6	$^3J_{3-4}$	$^5J_{3-6}$	$^3J_{4-5}$	$^3J_{5-6}$
1o	*trans*-PdR$_2$(tht)$_2$	*anti-Br,Br*	50	−127.8	−158.0	−156.8	−117.6	21.3	13.6	20.5	33.2
		syn-Br,Br	50	−127.3	−157.9	−156.7	−116.8	21.8	13.7	20.5	33.2
2o	*cis*-PdR$_2$(tht)$_2$	*anti-Br,Br*	72	−127.1	−159.1	−157.2	−114.2	21.2	11.3	19.4	32.0
		syn-Br,Br	28	−127.0	−159.2	−157.5	−112.0	21.2	11.2	19.7	31.9
3o	*cis*-PdR$_2$(COD)	*anti-Br,Br*	72	−126.5	−158.4	−156.8	−110.1	22.1	10.3	19.6	30.7
		syn-Br,Br	28	−126.4	−158.4	−156.9	−111.5	21.5	10.9	20.8	31.0
4o[c]	*trans*-PdR$_2$(PMe$_3$)$_2$	*anti-Br,Br*	50	−128.1	−159.1	−157.6	−116.0	20.8	13.6	19.2	33.5
		syn-Br,Br	50	−127.4	−159.1	−157.6	−115.4	20.8	13.4	19.2	33.4
5o[d]	*trans*-PdR$_2$(CNMe)$_2$			−129.3	−160.0	−158.7	−114.2	20.0		19.0	31.9
6o	*cis*-PdR$_2$(PMe$_3$)$_2$	*anti-Br,Br*	64	−128.0	−160.1	−157.7	−112.1	21.1		19.5	33.5
		syn-Br,Br	36	−127.5	−160.1	−158.0	−111.9	21.2	12.4	19.4	32.9
7o	*cis*-PdR$_2$(CNMe)$_2$	*anti-Br,Br*	56	−128.5	−160.0	−158.5	−112.5	21.1	10.8	19.4	30.2
		syn-Br,Br	44	−128.3	−160.0	−158.5	−112.5	21.3	11.4	19.4	30.8
8o	*cis*-PdR$_2$(Me$_2$bipy)	*anti-Br,Br*	55	−127.3	−159.9	−158.3	−112.5	21.4	11.3	19.5	30.8
		syn-Br,Br	45	−127.3	−159.9	−158.1	−111.9	21.3	11.7	19.5	31.6
9o	*cis*-PdR$_2$(OPPhPy$_2$)	*anti-Br,Br*	64	−125.5	−159.0	−157.9	−106.5	22.0	10.1	20.1	31.2
				−126.7	−159.3	−157.2	−108.2	22.0	10.1	20.1	31.2
		syn-Br,Br-anti-Br,P	28	−127.0	−159.5	−157.1	−111.3	22.0	10.1	20.1	30.9
		syn-Br,Br-syn-Br,P	8	−125.6	−159.6	−158.2	−109.3	22.0	10.1	20.1	
10o[d]	[PdR(μ-Cl)(tht)]$_2$	*trans*	81	−128.5	−158.2	−157.2	−119.2	20.5	9.8	18.9	29.2
		cis	19	−129.1	−162.5	−160.9	−118.1				
11o[e]	*trans*-PdRCl(tht)$_2$			−126.5	−157.0	−155.5	−118.0	21.0	10.9	19.3	30.3

[a] At 282 MHz, $CDCl_3$, 293 K: δ in ppm from $CFCl_3$; J in Hertz. [b] R = *o*-C_6F_4Br. [c] *anti-Br,Br*, $^4J_{6-P} = 4.8$ Hz, $^6J_{4-P} = 2.6$ Hz; *syn-Br,Br*, $^4J_{6-P} = 5.7$ Hz, $^6J_{4-P} = 2.6$ Hz. [d] In acetone-d_6, only one atropisomer at room temperature. [e] $^4J_{3-5} = 1.7$ Hz.

Table 2. ^{19}F NMR Data for (*m*-Bromotetrafluorophenyl)palladium(II) Complexes[a]

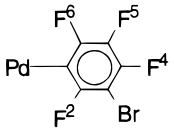

no.	complex[b]	atropisomer	%	δ_2	δ_4	δ_5	δ_6	$^5J_{2-5}$	$^3J_{4-5}$	$^3J_{5-6}$
1m	*trans*-PdR$_2$(tht)$_2$	*anti-Br,Br*	50	−89.5	−130.8	−161.6	−113.3	12.4	20.3	31.7
		syn-Br,Br	50	−89.5	−130.8	−161.6	−113.3	12.4	20.3	31.7
2m	*cis*-PdR$_2$(tht)$_2$	*anti-Br,Br*	52	−87.2	−131.9	−162.3	−110.7	*flux.*	*flux.*	*flux.*
		syn-Br,Br	48	−87.3	−131.9	−162.3	−110.7	*flux.*	*flux.*	*flux.*
3m[c]	*cis*-PdR$_2$(COD)	*anti-Br,Br*	52	−88.9	−131.0	−161.7	−111.5			
		syn-Br,Br	48	−89.1	−131.0	−161.6	−111.6	10.2	21.6	30.7
4m	*trans*-PdR$_2$(PMe$_3$)$_2$	*anti-Br,Br*	50	−88.0	−132.1	−162.4	−111.7	12.4	20.5	32.3
		syn-Br,Br	50	−88.0	−132.1	−162.5	−111.7	12.5	20.5	32.4
5m[d]	*trans*-PdR$_2$(CNMe)$_2$			−85.7	−132.7	−163.4	−109.6	11.4	21.0	31.5
6m	*cis*-PdR$_2$(PMe$_3$)$_2$	*anti-Br,Br*	*e*	−87.2	−133.0	−162.8	−110.6			
		syn-Br,Br	*e*	−87.3	−133.0	−162.9	−110.7	11.5	20.1	31.6
7m	*cis*-PdR$_2$(CNMe)$_2$			−87.4	−132.7	−163.6	−110.6	9.6	21.1	29.6
8m[d]	*cis*-PdR$_2$(Me$_2$bipy)	*anti-Br,Br*	50	−85.0	−133.6	−163.9	−109.2	10.7	20.4	31.9
		syn-Br,Br	50	−85.1	−133.6	−163.8	−109.1	11.7	20.6	30.1
9m[c]	*cis*-PdR$_2$(OPPhPy$_2$)	*anti-Br,Br*	54	−85.2	−132.1	−161.8	−112.3	10.3	21.8	30.9
				−88.6	−132.1	−162.3	−109.9	10.3	21.8	30.9
		syn-Br,Br-anti-Br,P	27	−89.3	−132.2	−162.6	−109.2	9.7	21.8	30.9
		syn-Br,Br-syn-Br,P	19	−86.1	−132.1	−162.1	−111.5	9.7	21.8	30.9
10m	[PdR(μ-Cl)(tht)]$_2$	*trans-anti-Br,Br*	35	−91.9	−129.9	−161.7	−115.1	9.0	20.8	28.3
		trans-syn-Br,Br	35	−91.9	−129.9	−161.7	−115.1	9.0	20.8	28.3
		cis-anti-Br,Br[g]	15	−91.7	−129.8	−161.5	−114.8			
		cis-syn-Br,Br[g]	15	−91.7	−129.8	−161.5	−114.8			
11m[f]	*trans*-PdRCl(tht)$_2$			−90.2	−129.8	−161.1	−113.7	10.3	20.8	29.4

[a] At 282 MHz, $CDCl_3$, 293 K: δ in ppm from $CFCl_3$; J in Hz. [b] R = *m*-C_6BrF_4. [c] At 233K. [d] In acetone-d_6. [e] Signals overlap. [f] $^3J_{2-4} = 2.9$ Hz, $^5J_{2-6} = 4.0$ Hz, $^4J_{4-6} = 3.4$ Hz. [g] Broad signals.

tives with one aryl group per palladium were prepared: [Pd$_2$R$_2$(μ-Cl)$_2$(tht)$_2$] (R = *o*-C_6BrF_4 (**10o**), *m*-C_6BrF_4 (**10m**)) were made by transarylation between [PdR$_2$(tht)$_2$] and $PdCl_2$ (eq 5). Cleavage of the chloro-bridges by tht afforded *trans*-[PdRCl(tht)$_2$] (**11o**, **11m**, eq 6).[10,11]

$$[PdR_2(tht)_2] + PdCl_2 \rightarrow [Pd_2R_2(\mu\text{-}Cl)_2(tht)_2] \quad (5)$$

$$[Pd_2R_2(\mu\text{-}Cl)_2(tht)_2] + 2tht \rightarrow 2\textit{trans}\text{-}[PdRCl(tht)_2] \quad (6)$$

Characterization of the Complexes and NMR Analysis. The complexes were characterized by el-

(11) Usón, R.; Forniés, J.; Navarro, R.; García, M. P. *Inorg. Chim. Acta* **1979**, *33*, 69−75.

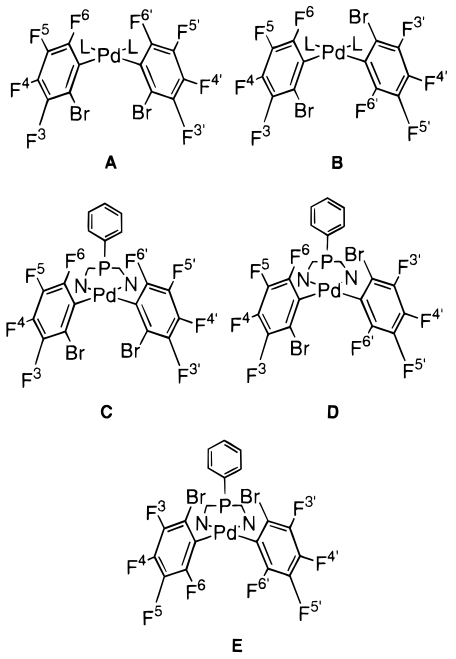

Figure 1. Structural formulae for atropisomers of complexes *cis*-[Pd(*o*-$C_6BrF_4)_2L_2$]: **A**, *cis-syn-Br,Br*-[Pd(*o*-$C_6BrF_4)_2L_2$]; **B**, *cis-anti-Br,Br*-[Pd(*o*-$C_6BrF_4)_2L_2$]; **C**, *cis-syn-Br,Br-anti-Br,P*-[Pd(*o*-$C_6BrF_4)_2$(OPPy$_2$Ph)]; **D**, (±)-*cis-anti-Br,Br*-[Pd(*o*-$C_6BrF_4)_2$(OPPy$_2$Ph)]; **E**, *cis-syn-Br,Br-syn-Br,P*-[Pd(*o*-$C_6BrF_4)_2$(OPPy$_2$Ph)].

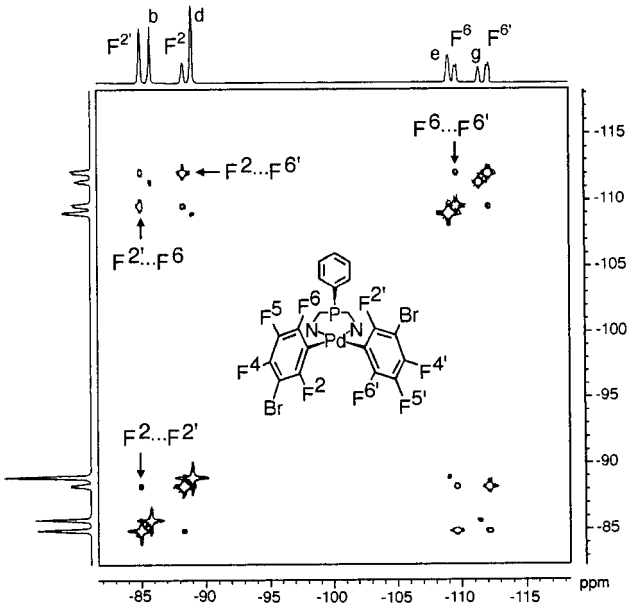

Figure 2. ^{19}F 282 MHz COSY ($CDCl_3$, F^2 and F^6 regions, 233 K) of *cis*-[Pd(*m*-$C_6BrF_4)_2$(OPPhPy$_2$)] (**9m**). The cross peaks between the $F^{2'}$−F^6, $F^{2'}$−F^2, F^2−$F^{6'}$, and F^6−$F^{6'}$ signals of the (±)-*anti-Br,Br* isomer reveal inter-ring couplings (indicated with arrows). The other signals are F^2 and $F^{2'}$ (b) and F^6 and $F^{6'}$ (g), corresponding to the *syn-Br,Br-syn-Br,P* isomer; F^2 and $F^{2'}$ (d) and F^6 and $F^{6'}$ (e), arising from the *syn-Br,Br-anti-Br,P* isomer.

emental analysis and IR and ^{1}H, ^{19}F, and ^{31}P NMR techniques. Relevant data are collected in the Experimental Section and in Tables 1 and 2.

Neither ^{1}H nor ^{31}P NMR spectra were useful for identification of the atropisomers in solution because of coincidence of resonances. The relative orientation of the C_6BrF_4 groups exerts little influence on the chemical shifts of the other ligands. However, ^{19}F NMR spectroscopy is extremely precise for the detection and identification of the atropisomers formed.

The simplest ^{19}F spectral pattern is found in the mono-arylated derivatives, **11o** and **11m**. Assignments of the different ^{19}F signals for these complexes were made using ^{19}F−^{19}F-COSY and homonuclear ^{19}F-decoupling experiments. In this way, chemical shift values and intra−ring ^{19}F−^{19}F scalar coupling constants could be determined and then used in the analysis of the more complex spectra of the bis-arylated derivatives. The scalar coupling constants connecting mutually *meta* ^{19}F nuclei are very small, hence the signals appear as doublets of doublets. The ^{19}F chemical shifts follow the order $\delta_F{}^6 > \delta_F{}^3 > \delta_F{}^5 > \delta_F{}^4$ in *o*-C_6BrF_4 complexes and $\delta_F{}^2 > \delta_F{}^6 > \delta_F{}^4 > \delta_F{}^5$ in *m*-C_6BrF_4 complexes. For each C_6BrF_4 group, only small changes in the chemical shifts (less than 3−4 ppm) are observed upon change of the ancillary ligand.

In the complexes *trans*-[Pd($C_6BrF_4)_2L_2$], both C_6BrF_4 groups (whether *ortho* or *meta*) are chemically equivalent. Two atropisomers are present, *syn-Br,Br* and *anti-Br,Br*, and two independent four-nuclei first-order spin systems are observed (one for each atropisomer), showing that there is no noticeable inter-ring coupling. Although the signals overlap, the analysis of the two overlapped systems can be made from their fine structure. The only exceptions are **5o** and **5m** for which only one isomer is observed at room temperature (Tables 1 and 2).

The *cis*-[Pd($C_6BrF_4)_2L_2$] complexes are not that simple. Even in the cases where the two C_6BrF_4 group are chemically equivalent, their fluorine atoms become magnetically inequivalent due to the existence of strong inter-ring ^{19}F−^{19}F coupling and an eight spin system must be considered. Such inter-ring couplings are clearly seen in the ^{19}F COSY spectrum of the *anti*-Br,-Br isomer of complex **9m** (Figure 2), where the F_{ortho} nuclei on different inequivalent *m*-C_6BrF_4 rings are coupled to each other giving the following cross peaks: F^2−$F^{6'}$ and $F^{2'}$−F^6 (same side of the coordination plane, *close* coupling); and F^2−$F^{2'}$ and F^6−$F^{6'}$ (opposite sides, *distant* coupling). In the case of the *anti-Br,Br* isomer of complex **9o**, only the distant coupling F^6−$F^{6'}$ is observed. Since the isomers *anti-Br,Br* of complexes **9** are asymmetric, both rings become inequivalent, providing a ^{19}F first-order spin system. Consequently, simple homodecoupling experiments allow one to measure of the inter-ring ^{19}F−^{19}F coupling constants (Table 3).

The assignment of the F^2 signals for both the *syn-Br,Br* atropisomers of complexes **9** is made on electronic and steric arguments: The higher frequency F^2 resonance is assigned to the *syn-Br,Br-syn-Br,P* isomer because of the anisotropic shielding of the close Ph group and because it is the less abundant one, in agreement with the higher sterically hindrance. The lower F^2 signal is assigned to the *syn-Br,Br-anti-Br,P* isomer.

The rest of the *cis* complexes, including the *syn-Br,-Br* atropisomers of complexes **9**, have at least one element of symmetry, and generate second order spins systems $F^3F^{3'}F^4F^{4'}F^5F^{5'}F^6F^{6'}$ (for the *ortho* isomer) or $F^2F^{2'}F^4F^{4'}F^5F^{5'}F^6F^{6'}$ (for the *meta* isomer), where F^n and $F^{n'}$ now stand for chemically equivalent but magneti-

(12) Usón, R.; Forniés, J.; Navarro, R; Gallo, A. *Transition Met. Chem.* **1980**, *5*, 284−288.

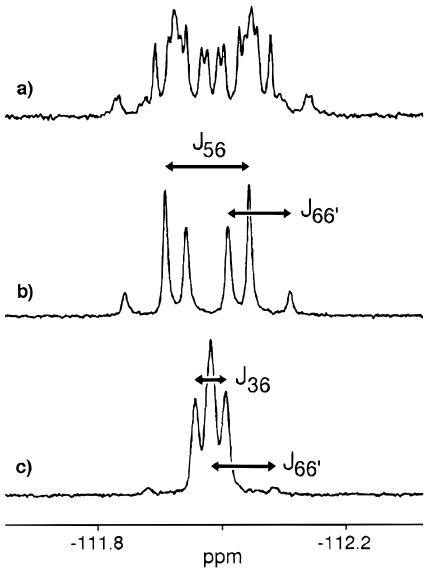

Figure 3. ^{19}F 282 MHz NMR spectra ($CDCl_3$, F^6 region) for *cis-syn-Br,Br*-[Pd(*o*-C_6BrF_4)$_2$(tht)$_2$] (**2o**). (a) Initial signal; (b) signal under F^3,$F^{3'}$ irradiation; (c) signal under F^5,$F^{5'}$ decoupling. Analysis of spectra b and c allows the determination of through-space $^{19}F-^{19}F$ coupling constants $J_{6-6'}$.

Table 3. $^{19}F-^{19}F$ Inter-Ring Couplings in *cis*-Bis(bromotetrafluorophenyl)palladium(II) Complexes[a]

no.	atropisomer	F···F close	*J*/Hz	F···F distant	*J*/Hz
2o	*syn-Br,Br*	$F^6-F^{6'}$	23.9		
	anti-Br,Br			$F^6-F^{6'}$	3.0
3o	*syn-Br,Br*	$F^6-F^{6'}$	52.0		
	anti-Br,Br			$F^6-F^{6'}$	<3
7o	*syn-Br,Br*	$F^6-F^{6'}$	22.5		
	anti-Br,Br			$F^6-F^{6'}$	3.7
8o	*syn-Br,Br*	$F^6-F^{6'}$	25.6		
	anti-Br,Br			$F^6-F^{6'}$	4.0
9o	*anti-Br,Br*			$F^6-F^{6'}$	<2
	syn-Br,Br-anti-Br,P	$F^6-F^{6'}$	50.9		
9m	*anti-Br,Br*			$F^2-F^{2'}$	3.3
				$F^6-F^{6'}$	3.3
		$F^2-F^{6'}$	25.5		
		$F^{2'}-F^6$	11.9		
	syn-Br,Br-anti-Br,P	$F^2-F^{2'}$	26.9		
		$F^6-F^{6'}$	9.9		
	syn-Br,Br-syn-Br,P	$F^2-F^{2'}$	13.2		
		$F^6-F^{6'}$	26.2		

[a] At 282 MHz, $CDCl_3$.

cally inequivalent nuclei. The measurement of the inter-ring $^{19}F-^{19}F$ coupling constants is not simple in this case. Fortunately, scalar couplings between mutually *meta* ^{19}F nuclei within the *o*-C_6BrF_4 rings are close to zero (in fact, the selective decoupling of F^4 resonance does not alter the F^6 signal), so the spin system involving F^6,$F^{6'}$ nuclei can be rewritten as $F^3F^{3'}F^5F^{5'}F^6F^{6'}$. This six-spin system can be further reduced to just four by using selective irradiation of a chosen F^3 or F^5 signal, giving AA′XX′ patterns that are easy to analyze (Figure 3). Some values of inter-ring coupling constants could be measured in this way (Table 3).

The approach just described is difficult to apply to the complexes *cis*-[Pd(*m*-C_6BrF_4)$_2$$L_2$]. The scalar coupling between mutually *meta* ^{19}F nuclei for these derivatives, $^4J_{2-6}$, although small (3−4 Hz), cannot be neglected, and the second-order spin systems cannot be simplified. Only for the *syn-Br,Br* isomers of **9m** (for which $^4J_{2-6}$ turned out to be smaller) could we estimate inter-ring coupling constants (Table 3).

The analysis of the ^{19}F spectra reveals the occurrence in the *cis* complexes of inter-ring F−F couplings ranging from very small to 52 Hz. Through-space coupling has been interpreted as a result of direct overlap of two lone-pair orbitals of close fluorine atoms giving rise to a bonding and an antibonding molecular orbital delocalized over both fluorine atoms; although there is no net F−F bonding, nuclear spin information is transmitted through this interaction.[4g] When two fluoroaryl groups are bound to a metal in a *cis* arrangement, the *syn* F_{ortho} atoms of both groups are very close to each other and the orbital interaction just described becomes very significant. This coupling sometimes leads to complicated spin systems, but on the other hand, it is very useful to identify the atropisomers formed in a *cis*-bis(aryl) complex. Thus, *syn-Br,Br* and *anti-Br,Br* atropisomers of the *cis*-[Pd(*o*-C_6BrF_4)$_2$$L_2$] derivatives are easily distinguished since the former shows a large inter-ring $F^6-F^{6'}$ coupling while the latter does not. The same applies to *cis*-[Pd(*m*-C_6BrF_4)$_2$$L_2$] derivatives: The *anti-Br,Br* atropisomer shows strong inter-ring coupling between the chemically inequivalent *syn* $F^2-F^{6'}$ atoms, while the *syn* atropisomer, with chemically equivalent *syn* $F^2-F^{2'}$ or $F^6-F^{6'}$ atoms, lacks this coupling.

The probable scalar contribution to the inter-ring coupling between F_{ortho} atoms can be estimated in **9o** (Table 3), where these *anti* atoms are too distant to expect a significant through-space contribution. This $^6J_{F-F}$ is found to be small (<2 Hz), as also confirmed by the value found for **9m** (3.3 Hz). Thus, most of the contribution found for *syn* F_{ortho} atoms is probably to be attributed to through-space coupling.

The magnitude of the through-space coupling is correlated with the nonbonding F···F distance.[4a] In these *cis* complexes, the values of close $F_{ortho}-F_{ortho}$ couplings range from 52 to 9.9 Hz (Table 3), which would correspond to F···F distances ranging from about 265 to about 320 pm. These distances are reasonable for the geometry of the complexes but reveal the existence of distortions of an ideally square-planar coordination with the two aryl rings perpendicular to the coordination plane. The highest values are observed for the *syn-Br,Br* atropisomers of **9o** (L = $OPPy_2Ph$) and **3o** (L = COD), and this can be explained assuming that the crowding in the *z* axis of two *syn ortho*-bromine atoms and the nonplanar ligands forces a tilt of the aryl groups in order to increase the distance between Br atoms, placing the *syn* F_{ortho} atoms closer to each other. Lower *J* values ranging from 25.6 to 22.5 Hz are found for the *syn-Br,Br* atropisomers of the other *o*-C_6BrF_4 derivatives involving ligands with no steric demand in the *z* axis (tht, CNMe, Me_2bipy).

Two different *close* $F_{ortho}-F_{ortho}$ coupling constants are found for each atropisomer of the *m*-C_6BrF_4 derivative **9m**, one medium and one small (26.2 and 13.2 Hz for the *syn-Br,Br* isomer; 26.9 and 9.9 Hz for the *anti-Br,Br*), supporting the existence of a tilt distortion of the aryl groups. It seems that the *meta*-Br atoms do not produce severe steric hindrance since, regardless their position, the F_{ortho} atoms close to the capping phenyl group of the ligand are the ones tilted away.

Although the distortions just discussed can explain the observations made, it must be kept in mind that

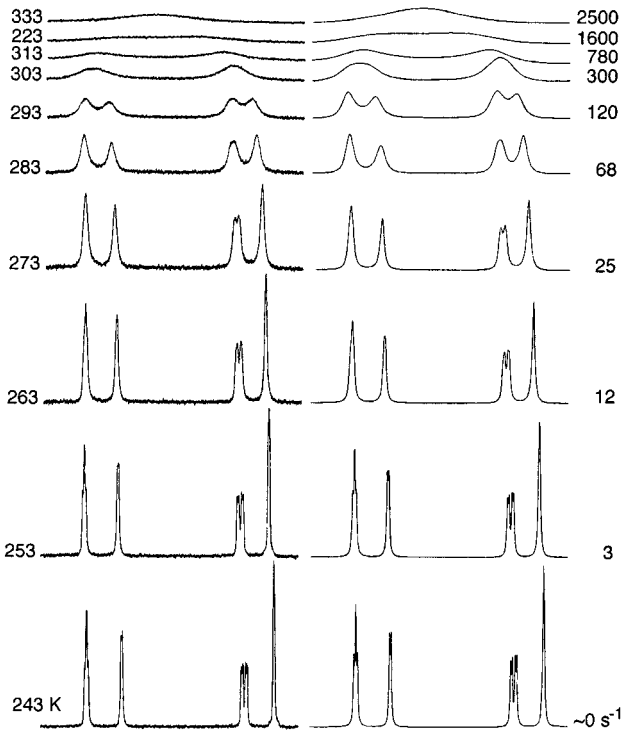

Figure 4. Experimental and simulated (DNMR6 program) ^{19}F 282 MHz NMR spectra ($CDCl_3$, F^2 region) for *cis*-[Pd(*m*-C_6BrF_4)$_2$($OPPy_2Ph$)] (**9m**). First-order atropisomerization constants (k_{atrop}) obtained by line shape analysis are given at each temperature. See Figure 2 for signal assignment.

other probable distortions, such as variations in the R−Pd−R angle, elongations of the Pd−R bonds, or out-of-plane tilting of the R group, are probably occurring to relieve inter-ring repulsions, particularly in the *o*-C_6BrF_4 derivatives.

Atropisomerization. In our previous study, we showed that k_{rot} depends on the "in-plane" size of the ligands flanking the C_6F_5 group in the coordination plane.[1] The results obtained here by ^{19}F NMR spectroscopy in $CDCl_3$ solution within the accessible temperature range (230−330 K) support this observation.

The *m*-C_6BrF_4 group seems to be sterically equivalent to C_6F_5 as far as rotation is concerned. For L = CNMe, the rotation is very fast and no atropisomers are observed even at low temperature. This is the less-hindered rotation. For the bulky (in the plane) L_2 = Me_2bipy, $2PMe_3$, the most hindered situations are observed, whereas slow rotations are observed for L_2 = COD, $OPPy_2Ph$, 2tht. A low-temperature ^{19}F NOESY of complex **9m** shows that chemical exchange affects all three atropisomers. Aryl group rotation is the only process that can bring about the simultaneous interconversion of every atropisomer, so this experiment unequivocally identifies the fluxional process operating. Line shape analysis was applied to variable-temperature ^{19}F spectra for complex **9m**. Simulation of the F^2 subspectra (Figure 4) was carried out using the DNMR6 program (see Experimental Section).[13,14] Atropisomerization rate constants, k_{atrop}, were found at different temperatures, and an Eyring plot gave the following activation parameters: $\Delta H^{\ddagger} = 56.2 \pm 1.2$ kJ mol^{-1} and $\Delta S^{\ddagger} = -12 \pm 4$ J K^{-1} mol^{-1}. These values are very similar to those values found for C_6F_5 rotation in [$Pd(C_6F_5)_2(OPPy_2Ph)$] ($\Delta H^{\ddagger} = 52.7$ kJ mol^{-1}, $\Delta S^{\ddagger} = -18.2$ J K^{-1} mol^{-1}), supporting that *m*-C_6BrF_4 and C_6F_5 are sterically equivalent as far as rotation is concerned.

Atropisomerization also occurs for the *o*-C_6BrF_4 derivatives, but at a much slower rate. Thus, for **9o** at 323 K, only broadening, but still no coalescence of the ^{19}F signals, is observed. In fact, all of the complexes show two atropisomers at room temperature, except **5o** which shows only one with broad lines and can be resolved in two at lower temperatures ($\Delta G^{\ddagger}_{283} = 55.8$ kJ mol^{-1}). The differences in the energy of activation between the analogous derivatives of *o*-C_6BrF_4 and *m*-C_6BrF_4 must be related to the bulkiness of the *ortho*-Br compared to the F substituent. Moreover, the fact that **5o** and **7o**, both having the aryl group flanked by one C atom in the coordination plane, present very different rotation barriers reveals that for the *o*-C_6BrF_4 derivatives this simplification is not valid and the bulk of the Br substituent in the direction perpendicular to the coordination plane is the main hindrance to rotation in the *cis* isomer.

Experimental Section

All reactions involving organolithium reagents or PMe_3 were carried out under dinitrogen atmosphere. Commercial reagents were used without further purification. Solvents were freshly distilled from standard drying agents. Methyl isocyanide (CNMe, used as a dichloromethane solution previously titrated by ^{1}H NMR using 4-bromoanisol as an internal standard),[15] bis(2-pyridyl)phenylphosphine-*P*-oxide ($OPPy_2Ph$),[16] *cis*-[$PdCl_2$(COD)],[17] and *trans*-[$PdCl_2$(tht)$_2$][18] were prepared as described in the literature. Infrared spectra (KBr pellets or Nujol mull) were recorded on a Perkin-Elmer FT1720X spectrophotometer. Elemental C, H, and N analyses were carried out on a Perkin-Elmer 2400 CHN microanalyzer. NMR spectra were recorded on a Bruker ARX 300 spectrometer (300 MHz for ^{1}H; 282 MHz for ^{19}F; 121 MHz for ^{31}P) equipped with a VT-100 variable-temperature unit. Temperature calibration was performed before measurements using the temperature-dependent chemical shift differences of the ^{1}H resonances of methanol (below room temperature) or ethylene glycol (high temperatures). Chemical shifts are reported as δ (ppm) from TMS, CCl_3F, or H_3PO_4.

LiR solutions (R = *o*-C_6BrF_4, *m*-C_6BrF_4). To a stirred solution of 1,2-$C_6Br_2F_4$ (1.92 g, 6.22 mmol) in dry diethyl ether (40 mL) at −78 °C was added dropwise, over a period of 25 min, a solution of Li^{n}Bu (6.22 mmol) in Et_2O (20 mL), prepared by dilution of a commercial solution (1.6 M in *n*-hexane). A green solution of Li(*o*-C_6BrF_4) was obtained, and it was stirred for an additional 20 min at −78 °C before being reacted with the corresponding palladium complex (see below). Solutions of Li(*m*-C_6BrF_4) (pale pink) were prepared in the same way starting from 1,3-$C_6Br_2F_4$.

(13) *DNMR6; Quantum Chemical Program Exchange (QCPE 633)*; Indiana University, Bloomington, IN, 1995.

(14) The equilibrium between atropisomers shows a small dependence on temperature. Thus, as temperature raises, the ratio of atropisomers for complex **9m** changes slightly and approaches to the statistical distribution: *syn-Br,Br-syn-Br,P*:*syn-Br,Br-anti-Br,P*:*anti-Br,Br* (two enantiomers) = 19:27:54 (243 K); *syn-Br,Br-syn-Br,P*:*syn-Br,Br-anti-Br,P*:*anti-Br,Br* (two enantiomers) = 25:25:50 (323 K). Since the populations of four sites are very close (*ca.* 25%), we assumed identical atropisomerization rates between every pair of syn−anti conformations.

(15) Weber, W. P.; Gokel, G. W.; Ugi, I. K. *Angew. Chem., Int. Ed. Engl.* **1972**, *11*, 530−531.

(16) (a) $OPPy_2Ph$: Newcome, G.; Hagen, D. C. *J. Org. Chem.* **1978**, 947−949. (b) PPy_2Ph: Espinet, P.; Gómez-Elipe, P.; Villafañe F. *J. Organomet. Chem.* **1993**, *450*, 145−150.

(17) Drew, D.; Doyle, J. R. *Inorg. Synth.* **1972**, *13*, 52−53.

(18) Usón, R.; Forniés, J.; Martinez, F.; Tomás, M. *J. Chem. Soc., Dalton Trans.* **1980**, 888−894.

[PdR_2(tht)$_2$] (*trans* R = *o*-C_6BrF_4 (1o), *m*-C_6BrF_4 (1m), *cis* R = *o*-C_6BrF_4 (2o), *m*-C_6BrF_4 (2m)). To a Li(*o*-C_6BrF_4) (6.22 mmol) solution in Et_2O (60 mL) at −78 °C was added finely ground *trans*-[$PdCl_2$(tht)$_2$] (1.000 g, 2.828 mmol). The mixture was stirred for 15 min at −78°C, and then the temperature was allowed to increase slowly for 40 min, 2 drops of distilled water were added, and it was evaporated to dryness. The residue was extracted with dichloromethane (80 mL) to give a yellow solution; the CH_2Cl_2 solution was evaporated to *ca*. 5 mL. Ethanol (5 mL) was added, and the mixture was cooled to −28 °C and let stand for 3 h to give pale yellow crystals, which were filtered, washed with cold ethanol (2 × 5 mL), and air-dried (1.810 g, 87% crude yield). The crystals were a mixture of isomers **1o** and **2o** which were separated in two steps: First, fractional crystallization in dichloromethane at −28 °C leading to two batches of pure isomers and an intermediate crop containing the isomeric mixture. The latter was column chromatographed (silicagel neutral 60 mesh, CH_2Cl_2:*n*-hexane = 1:5). After separation, pure *trans*-[Pd(*o*-C_6BrF_4)$_2$(tht)$_2$] (**1o**) (1.358 g, 63%) and *cis*-[Pd(*o*-C_6BrF_4)$_2$(tht)$_2$] (**2o**) (0.181 g, 11%) were obtained. **1o**: IR (cm^{-1}, KBr) 1484 (vs), 1421 (vs), 1080 (vs), 1003 (vs), 814 (vs), 754 (vs); ^{1}H NMR ($CDCl_3$, 293 K) δ 2.69 (m, SCH_2), 1.89 (m, CCH_2). Anal. Calcd for $C_{20}H_{16}Br_2F_8PdS_2$: C, 32.52; H, 2.18. Found: C, 32.43; H, 2.22. **2o**: IR (cm^{-1}, KBr) 1485 (vs), 1423 (vs), 1086 (vs), 1008 (vs), 817 (vs), 767 (vs); ^{1}H NMR ($CDCl_3$, 293 K) δ 2.90 (m, SCH_2), 1.95 (m, CCH_2). Anal. Calcd for $C_{20}H_{16}Br_2F_8PdS_2$: C, 32.52; H, 2.18. Found: C, 32.63; H, 2.17. Complexes *trans*-[Pd(*m*-C_6BrF_4)$_2$(tht)$_2$] (**1m**) (25%) and *cis*-[Pd(*m*-C_6BrF_4)$_2$(tht)$_2$] (**2m**) (20%) were obtained similarly using Li(*m*-C_6BrF_4). **1m**: IR (cm^{-1}, KBr) 1466 (vs), 1413 (vs), 1052 (vs), 1023 (vs), 871 (vs), 723 (w), 658 (s); ^{1}H NMR ($CDCl_3$, 293 K) δ 2.68 (m, SCH_2), 1.85 (m, CCH_2). Anal. Calcd for $C_{20}H_{16}Br_2F_8PdS_2$: C, 32.52; H, 2.18. Found: C, 32.56; H, 2.06. **2m**: IR (cm^{-1}, KBr) 1466 (vs), 1420 (vs), 1051 (vs), 872 (vs), 723 (w), 669 (m); ^{1}H NMR ($CDCl_3$, 293 K) δ 2.88 (m, SCH_2), 1.87 (m, CCH_2). Anal. Calcd for $C_{20}H_{16}Br_2F_8PdS_2$: C, 32.52; H, 2.18. Found: C, 32.21; H, 2.09.

***cis*-[PdR_2(COD)] (R = *o*-C_6BrF_4 (3o), *m*-C_6BrF_4 (3m)). Method A.** To a Li(*o*-C_6BrF_4) solution (6.30 mmol) at −78 °C, prepared as described above, finely ground *cis*-[$PdCl_2$-(COD)] was added (1.000 g, 2.828 mmol). The cool bath was removed, and the mixture was stirred for 2 h while the temperature increased. The resulting suspension was treated with 2 drops of distilled water and evaporated to dryness. The residue was extracted with dichloromethane (100 mL) to give a yellow solution that was then evaporated to ca. 2 mL. Ethanol (5 mL) was added, and the mixture was cooled to −28 °C and let stand for 3 h. A crystalline pale yellow solid was obtained, *cis*-[Pd(*o*-C_6BrF_4)$_2$(COD)] (**3o**), which was then filtered out, washed with cold ethanol (3 × 1 mL), and air-dried (1.138 g, 60%). **Method B.** To a Li(*o*-C_6BrF_4) solution (6.30 mmol) at −78 °C, prepared as described above, finely ground *cis*-[$PdCl_2$(COD)] was added (1.000 g, 2.828 mmol). The mixture was stirred overnight (*ca*. 17 h) while the bath temperature raised slowly. The resulting suspension was treated with 2 drops of distilled water and evaporated to dryness. The residue was extracted with dichloromethane (100 mL) to give a green-yellow solution that was evaporated to *ca*. 5 mL. Crystallization at −28 °C for 2 h yielded a yellow solid [Pd_2(μ-Cl)$_2${6-(*o*-C_6BrF_4)-η^3-cyclooct-1-en-5-yl}$_2$] (**12**), which was filtered, washed with cold dichloromethane (2 × 4 mL), and air-dried (0.4926 g, 26%). The mother liquors were then evaporated to dryness, ethanol (5 mL) was added, and the mixture was cooled to −28 °C. After 3 h a pale greenish solid crystallized, which was a mixture of **3o** and **12**. It was filtered, washed with cold ethanol (3 × 2 mL), and air-dried (0.777 g, 41% crude yield). The mixture was then column chromatographed (silicagel neutral 60 mesh, CH_2Cl_2:*n*-hexane = 1:5), giving pure pale yellow *cis*-[Pd(*o*-C_6BrF_4)$_2$(COD)] (**3o**) (0.606 g, 32%). **3o**: IR (cm^{-1}, KBr) 1484 (vs), 1419 (vs), 1089 (vs), 1008 (vs), 820 (vs), 766 (vs); ^{1}H NMR ($CDCl_3$, 293 K) δ 5.95 (m, =CH), 5.90 (m, =CH), 2.87 (m, CCH_2), 2.85 (m, CCH_2). Anal. Calcd for $C_{20}H_{12}Br_2F_8Pd$: C, 35.83; H, 1.80. Found: C, 35.72; H, 1.70. **12**: IR (cm^{-1}, KBr) 1504 (vs), 1462 (vs), 1113 (s), 1064 (s), 946 (s), 817 (s), 277, 260 cm^{-1} (m, Pd−Cl); ^{1}H NMR ($CDCl_3$, 293 K) δ 6.14 (bs, 2H, =CH), 5.59 (bs, 2H, =CH), 3.66 (d, J = 13 Hz, 2H, PdCH), 3.39 (bs, 2H), 2.96 (m, 2H), 2.69 (m, 4H), 2.38 (m, 6H), 1.95 (d, 13 Hz, 2H, PdCCH), 1.27 (m, 2H); ^{19}F NMR ($CDCl_3$, 293 K) δ −125.6 (bd, J = 14 Hz, F^3), −137.2 (bd, J = 14 Hz, F^6), −156.0 (dd, J_{4-5} = 21.2 Hz, J_{5-6} = 20.2 Hz, F^5), −156.2 (dd, J_{3-4} = 20.3 Hz, J_{4-5} = 21.2 Hz, F^4). Anal. Calcd for $C_{28}H_{24}Br_2Cl_2F_8Pd_2$: C, 35.18; H, 2.53. Found: C, 34.88; H, 2.40. Complex *cis*-[Pd(*m*-C_6BrF_4)$_2$(COD)] (**3m**) (71%) was obtained following method A and using [Li(*m*-C_6BrF_4)]: IR (cm^{-1}, KBr) 1466 (vs), 1418 (vs), 1055 (vs), 874 (vs), 722 (w), 675 (m); ^{1}H NMR ($CDCl_3$, 293 K) δ 5.80 (s, =CH), 2.75 (s, CCH_2). Anal. Calcd for $C_{20}H_{12}Br_2F_8Pd$: C, 35.83; H, 1.80. Found: C, 35.71; H, 1.89.

***trans*-[PdR_2L_2] (R = *o*-C_6BrF_4, L = PMe_3 (4o), CNMe (5o); R = *m*-C_6BrF_4, L = PMe_3 (4m), CNMe (5m)).** To a solution of **1o** (0.100 g, 0.135 mmol) in dichloromethane (20 mL) was added a slight excess of PMe_3 (0.30 mL, 0.300 mmol), and the mixture was stirred for 30 min. The resulting solution was evaporated to dryness, and the residue was treated with ethanol (3 mL). This afforded white **4o**, which was washed with cold ethanol (2 × 1 mL) and air-dried (0.0781 g, 81%): IR (cm^{-1}, KBr) 1480 (vs), 1413 (vs), 1078 (vs), 1002 (vs), 814 (vs), 754 (vs); ^{1}H NMR ($CDCl_3$, 293 K) δ 1.40 (m, J = 3.5 Hz, CH_3), 1.11 (m, J = 3.5 Hz, CH_3); ^{31}P{^{1}H} NMR ($CDCl_3$, 293 K) δ −13.90 (s). Anal. Calcd for $C_{18}H_{18}Br_2F_8P_2Pd$: C, 30.26; H, 2.54. Found: C, 30.36; H, 2.44. Complexes **4m** (88%), **5o** (95%), and **5m** (95%) were prepared similarly. **4m**: IR (cm^{-1}, KBr) 1461 (vs), 1408 (vs), 1046 (vs), 1024 (vs), 866 (vs), 723 (w), 658 (s); ^{1}H NMR ($CDCl_3$, 293 K) δ 1.09 (m, J = 3.6 Hz, CH_3); ^{31}P{^{1}H} NMR ($CDCl_3$, 293 K) δ −13.12 (s). Anal. Calcd for $C_{18}H_{18}Br_2F_8P_2Pd$: C, 30.26; H, 2.54. Found: C, 30.46; H, 2.45. **5o**: IR (cm^{-1}, KBr) 2256 (vs, st CN), 1484 (vs), 1419 (vs), 1080 (vs), 1005 (vs), 818 (vs), 756 (vs); ^{1}H NMR (acetone-d_6, 293 K) δ 3.52 (s, CH_3). Anal. Calcd for $C_{16}H_6Br_2F_8N_2Pd$: C, 29.82; H, 0.94; N, 4.35. Found: C, 29.98; H, 1.15; N, 4.25. **5m**: IR (cm^{-1}, KBr) 2256 (vs, st CN), 1466 (vs), 1418 (vs), 1053 (vs), 1031 (vs), 872 (vs), 725 (m), 666 (s); ^{1}H NMR (acetone-d_6, 293 K) δ 3.55 (t, CH_3). Anal. Calcd for $C_{16}H_6Br_2F_8N_2Pd$: C, 29.82; H, 0.94; N, 4.35. Found: C, 30.02; H, 1.16; N, 4.84.

***cis*-[PdR_2L_2] (R = *o*-C_6BrF_4, L = PMe_3 (6o), CNMe (7o), $^1/_2$$Me_2$bipy (8o), $^1/_2$$OPPy_2$Ph (9o), tht (2o); R = *m*-C_6BrF_4, L = PMe_3 (6m), CNMe (7m), *1*/$_2$$Me_2$bipy (8m), $^1/_2$$OPPy_2$Ph (9m), tht (2m)).** To a solution of **3o** (0.100 g, 0.149 mmol) in dichloromethane (50 mL) was added PMe_3 (0.30 mL, 0.300 mmol), and the mixture was stirred for 30 min. The solution was evaporated to dryness, and the residue was triturated with *n*-hexane (3 mL). This afforded white *cis*-[Pd(*o*-C_6BrF_4)$_2$-(PMe_3)$_2$] (**6o**), which was washed with *n*-hexane (3 × 1 mL) and air-dried (0.096 g, 90%): IR (cm^{-1}, KBr) 1484 (vs), 1419 (vs), 1079 (vs), 1004 (vs), 812 (vs), 760 (vs); ^{1}H NMR ($CDCl_3$, 293 K) δ 1.33 (m, J_{H-P} = 8.54 Hz, CH_3), 1.31 (m, J_{H-P} = 8.54 Hz, CH_3); ^{31}P{^{1}H} NMR ($CDCl_3$, 293 K) δ −19.80 (bs, 2P), −20.3 (bs, 2P). Anal. Calcd for $C_{18}H_{18}Br_2F_8P_2Pd$: C, 30.26; H, 2.54. Found: C, 30.41; H, 2.77. Complexes **6m**, **7o**, **7m**, **8o**, **8m**, **9o**, **9m**, **2o**, and **2m** were prepared similarly in yields higher than 90% but using the suitable complex *cis*-[PdR_2-(COD)] (**3**) and ligand L (200% excess of tht was used for displacing COD). **6m**: IR (cm^{-1}, KBr) 1462 (vs), 1414 (vs), 1044 (vs), 867 (vs), 736 (m), 661 (m); ^{1}H NMR ($CDCl_3$, 293 K) δ 1.30 (m, J_{H-P} = 8.79 Hz, CH_3); ^{31}P{^{1}H} NMR ($CDCl_3$, 293 K) δ −18.77 (m). Anal. Calcd for $C_{18}H_{18}Br_2F_8P_2Pd$: C, 30.26; H, 2.54. Found: C, 30.36; H, 2.48. **7o**: IR (cm^{-1}, KBr) 2249 (vs, st CN), 1484 (vs), 1417 (vs), 1080 (vs), 1006 (vs), 822 (s), 761 (s); ^{1}H NMR ($CDCl_3$, 293 K) δ 3.38 (s, CH_3). Anal. Calcd for $C_{16}H_6Br_2F_8N_2Pd$: C, 29.82; H, 0.94; N, 4.35. Found: C, 30.21; H, 1.27; N, 4.22. **7m**: IR (cm^{-1}, KBr) 2241 (vs, st CN), 1462 (vs), 1420 (vs), 1053 (vs), 872 (vs), 724 (m), 668 (s); ^{1}H NMR ($CDCl_3$, 293 K) δ 3.38 (t, CH_3). Anal. Calcd for $C_{16}H_6Br_2F_8N_2$-

Pd: C, 29.82; H, 0.94; N, 4.35. Found: C, 30.16; H, 1.18; N, 4.72. **8o**: IR (cm^{-1}, KBr) 1484 (vs), 1418 (vs), 1083 (vs), 1006 (vs), 823 (s), 766 (s); ^1H NMR ($CDCl_3$, 293 K) δ 7.90 (s, *H*-Py), 7.80 (d, $J = 5.6$ Hz, *H*-Py), 7.78 (d, $J = 5.6$ Hz, *H*-Py), 7.25 (d, $J = 5.6$ Hz, *H*-Py), 7.22 (d, $J = 5.6$ Hz, *H*-Py), 2.53 (s, CH_3). Anal. Calcd for $C_{24}H_{12}Br_2F_8N_2Pd$: C, 38.61; H, 1.62; N, 3.75. Found: C, 39.00; H, 1.63; N, 3.68. **8m**: IR (cm^{-1}, KBr) 1462 (vs), 1418 (vs), 1056 (vs), 872 (vs), 724 (m), 675 (s); ^1H NMR (acetone-d_6, 293 K) δ 8.50 (s, *H*-Py), 7.92 (d, $J = 5.6$ Hz, *H*-Py), 7.47 (d, $J = 5.6$ Hz, *H*-Py), 2.57 (s, CH_3). Anal. Calcd for $C_{24}H_{12}Br_2F_8N_2Pd$: C, 38.61; H, 1.62; N, 3.75. Found: C, 39.01; H, 1.98; N, 3.59. **9o**: IR (cm^{-1}, KBr) 1485 (vs), 1419 (vs), 1086 (vs), 1010 (s), 821 (s), 766 (s); $^{31}P\{^1H\}$ NMR ($CDCl_3$, 293 K) δ 20.72 (s). Anal. Calcd for $C_{28}H_{13}Br_2F_8N_2OPPd$: C, 39.91; H, 1.56; N, 3.33. Found: C, 40.25; H, 1.91; N, 3.21. **9m**: IR (cm^{-1}, KBr) 1467 (vs), 1418 (vs), 1058 (vs), 1022 (vs), 872 (vs), 733 (s), 673 (s); $^{31}P\{^1H\}$ NMR ($CDCl_3$, 293 K) δ 20.26 (s). Anal. Calcd for $C_{28}H_{13}Br_2F_8N_2OPPd$: C, 39.91; H, 1.56; N, 3.33. Found: C, 40.26; H, 1.95; N, 3.04.

[Pd$_2$R$_2$(μ-Cl)$_2$(tht)$_2$] (R = *o*-C$_6$BrF$_4$ (10o), *m*-C$_6$BrF$_4$ (10m)). A mixture of **1o** (0.200 g, 0.271 mmol) and $PdCl_2$ (0.048 g, 0.271 mmol) was refluxed in acetone (30 mL) for 2 h. The resulting warm yellow solution was filtered through Celite and evaporated to dryness to give yellow **10o**, which was washed with diethyl ether, filtered, and air-dried (0.211 g, 85% yield): IR (cm^{-1}, KBr) 1489 (vs), 1434 (vs), 1092 (vs), 1012 (vs), 826 (vs), 776 (vs), 288 (s, st Pd−Cl); ^1H NMR (acetone-d_6, 293 K) δ 2.89 (bs, SCH_2), 2.06 (bs, CCH_2). Anal. Calcd for $C_{20}H_{16}Br_2Cl_2F_8S_2Pd_2$: C, 26.23; H, 1.76. Found: C, 26.16; H, 1.76. **10m** was prepared similarly from **1m** (81% yield): IR (cm^{-1}, KBr) 1471 (vs), 1424 (vs), 1061 (vs), 1046 (vs), 872 (vs), 726 (m), 676 (s), 292 (s, st Pd−Cl); ^1H NMR (acetone-d_6, 293 K) δ 2.95 (bs, SCH_2), 2.05 (bs, CCH_2). Anal. Calcd for $C_{20}H_{16}Br_2Cl_2F_8S_2Pd_2$: C, 26.23; H, 1.76. Found: C, 26.49; H, 1.84.

***trans*-[PdRCl(tht)$_2$] (R = *o*-C$_6$BrF$_4$ (11o), *m*-C$_6$BrF$_4$ (11m)).** To a suspension of **10o** (0.210 g, 0.230 mmol) in acetone (60 mL) was added tht (0.06 mL, 0.680 mmol). The resulting solution was stirred for 40 min and evaporated to dryness. The residue was triturated with *n*-hexane (5 mL) and stored at −28 °C for 2 h. Yellow *trans*-[Pd(*o*-C_6BrF_4)Cl(tht)$_2$] (**11o**) was obtained, which was filtered, washed with cold *n*-hexane (3 × 1 mL), and air-dried (0.153 g, 61%): IR (cm^{-1}, KBr) 1485 (vs), 1424 (vs), 1082 (s), 1010 (vs), 822 (vs), 768 (s), 303 (s, st Pd−Cl); ^1H NMR ($CDCl_3$, 293 K) δ 3.02 (bs, SCH_2), 2.01 (m, CCH_2). Anal. Calcd for $C_{14}H_{16}BrClF_4S_2Pd$: C, 30.79; H, 2.95. Found: C, 30.34; H, 2.71. **11m** was obtained from **10m** in similar yield: IR (cm^{-1}, KBr) 1467 (vs), 1423 (vs), 1062 (vs), 1060 (vs), 876 (vs), 725 (m), 675 (m), 314 (s, st Pd−Cl); ^1H NMR ($CDCl_3$, 293 K) δ 3.03 (bs, SCH_2), 2.02 (bs, CCH_2). Anal. Calcd for $C_{14}H_{16}BrClF_4S_2Pd$: C, 30.79; H, 2.95. Found: C, 30.48; H, 2.61.

Kinetic Studies on the Isomerization of *trans*-[PdR$_2$(tht)$_2$] (1o, 1m). NMR tubes (5 mm) were charged with $CDCl_3$ solutions (10^{-2} mol L^{-1}) of complexes **1o** or **1m** and placed into a thermostated probe at 318.2 K (± 0.2 K). Conversion(x)-time(t) data were then acquired from ^1H NMR SCH_2 signal areas for the *cis* and *trans* isomers and fitted to equation ln(x) *vs* t, getting first-order constants k_{iso} (standard errors are also given).

Simulation of NMR Spectra. First-order rate constants for atropisomerization k_{atrop} were obtained from line shape analysis by matching the observed variable-temperature ^{19}F NMR spectra for complex **9m** with those simulated using the DNMR6 program.[13] The temperature dependence of the chemical shifts was analyzed in the slow exchange region, and a linear dependence was found; δ values for the coalescence region were calculated according to this linear correlation and used in the simulation. The rate constant matrix was constructed assuming that the exchange rates which involve the concerted rotation of two rings are negligible, whereas exchange rates involving single rotations are of the same value. An Eyring plot of $\ln(k_{atrop}/T)$ *vs* $1/T$ was represented. Activation parameters, $\Delta H^{\ddagger}$ and $\Delta S^{\ddagger}$, were calculated from the slope and the intercept, respectively, of the best fit line drawn by a least-squares analysis. Uncertainties in the activation parameters were calculated from the uncertainties of the slope and the intercept of the best fit line.

Acknowledgment. We are very grateful to Dr. J. A. Casares and Dr. J. M. Martínez for helpful discussions. Financial support was granted by the Dirección General de Investigación Científica y Técnica (Project No. PB96-0363) and the Junta de Castilla y León (Project No. VA 40-96). The Ministerio de Educación y Ciencia is gratefully acknowledged for a fellowship to A.L.C.

OM970529D